THE JOURNAL OF NAVIGATION (2004), **57**, 85–101.
DOI: 10.1017/S0373463303002583 Printed in the United Kingdom

Development of an Integrated Low-Cost GPS/Rate Gyro System for Attitude Determination

Chaochao Wang, Gérard Lachapelle and M. Elizabeth Cannon

(*Department of Geomatics Engineering*, *University of Calgary*)

The use of low-cost GPS receivers and antennas for attitude determination can significantly reduce the overall hardware system cost. Compared to the use of high performance GPS receivers, the carrier phase measurements from low-cost equipment are subject to additional carrier phase measurement errors, such as multipath, antenna phase centre variation and noise. These error sources, together with more frequent cycle slip occurrences, severely deteriorate attitude determination availability, reliability and accuracy performance. This paper presents the investigation of a low-cost GPS/gyro integration system for attitude determination. By employing the dead reckoning sensor type, the ambiguity search region can be specifically defined as a small cube to enhance the ambiguity resolution process. A Kalman filter is implemented to fuse the rate gyro data with GPS carrier phase measurements. The quality control system based on innovation sequences is used to identify cycle slip occurrences and incorrect inter-antenna vector solutions. The availability of the integrated system also improves with respect to the GPS standalone system since the attitude parameters can be estimated using the angular rate measurements from rate gyros during GPS outages. The low-cost hardware used to design and test the integrated system consists of CMC Allstar receivers with the OEM AT575-70 antennas and Murata ENV-05D-52 piezoelectric vibrating rate gyroscopes. Tests in the urban area demonstrated that the introduction of rate gyros in a GPS-based attitude determination system not only effectively decreased the noise level in the estimated attitude parameters but coasted the attitude output during GPS outages and also significantly improved the system reliability.

KEY WORDS

1. Integrated System. 2. GPS. 3. Rate Gyro. 4. Attitude Determination.

1. INTRODUCTION. GPS attitude determination using multiple closely-spaced antennas has been extensively investigated in the past ten years and has proven to be a cost effective solution for attitude estimation without error drifting over time (e.g. Cohen 1992, Lu 1994). Most of the work has been done using high performance GPS hardware, largely to mitigate carrier phase measurement errors and to improve accuracy and reliability. In recent years, as low-cost GPS receivers that can output good quality time-synchronized carrier phase measurements appeared on the market, research has been initiated to investigate the feasibility of using this low cost hardware to improve cost effectiveness (Hoyle et al 2002, Gebre-Egziabher et al 1998). Due to hardware limitations, the carrier phase measurements from a

low-cost GPS receiver system are more vulnerable to such errors as multipath, antenna phase centre offsets and receiver noise. Previous research has shown that, even though low-cost GPS sensors can be used for attitude determination, the performance of such a low-cost system highly depends on the multipath environment and platform dynamics (Wang & Lachapelle 2002). In cases when strong multipath and large antenna phase centre variations exist, it takes a long time to solve the carrier phase integer ambiguities or incorrect ambiguities are resolved, which inevitably leads to erroneous attitude component estimates.

In order to improve the reliability of low-cost attitude systems, specific measures such as high data rate measurements, angular constraint checks and a quality control system in the Kalman filter, have been implemented by Wang and Lachapelle (2002) to detect incorrect carrier phase ambiguities and/or erroneous inter-antenna vector solutions. The above three schemes can successfully identify most of the erroneous antenna vector quasi-observables both in static and kinematic attitude applications. However, the use of statistical reliability analysis has shown the limitations of the above three techniques due to the presence of noisy carrier phase measurements and the lack of direct angular rate measurements in the Kalman filter. In the research presented here, three piezoelectric rate gyros, namely Murata ENV-05D-52 Gyrostar units, are used as sensors to monitor the angular rates around the three axes in the body frame. These rate gyros are selected for their low-cost (less than $15 per unit in large quantities) and their performance relative to other MEMS gyro sensors in the same price range. The angular rate measurements are fused with the estimated antenna vector components to estimate the attitude parameters as well as their angular rates in a centralized Kalman filter. By employing these low-cost gyros, the performance of attitude estimation can be improved in term of accuracy, availability and reliability. The integration methodologies are realized in a high performance, open architecture attitude determination software, namely HEADRT+^{TM}, developed at the University of Calgary (Hoyle et al 2002). A series of static and kinematic tests are presented to assess the performance of the integrated system under field conditions.

2. ATTITUDE DETERMINATION USING GPS.

The GPS sensors are primarily used to determine the inter-antenna vectors as well as the approximate positions of the platform in the navigation frame. Regardless of the platform dynamics, the relative positions of the multiple antennas in the body frame remain fixed and can be accurately measured during system installation. The attitude of the platform, which is the rotation of the body frame with respect to the local level frame, can then be precisely estimated, if and once the coordinates of the antennas in the local level frame have been correctly estimated by the GPS measurements. The three Euler attitude angles in the rotation matrix can be calculated as:

$$\begin{pmatrix} x^b \\ y^b \\ z^b \end{pmatrix} = R^b_{ll}(\psi, \theta, \varphi) \begin{pmatrix} x^{ll} \\ y^{ll} \\ z^{ll} \end{pmatrix} \tag{1}$$

where ψ, θ, φ denote heading, pitch and roll, x, y, z are the cartesian coordinates of the antenna vector, the superscript b represents the body frame, and the superscript

https://doi.org/10.1017/S0373463303002583 Published online by Cambridge University Press

ll stands for the local level frame. The carrier phase measurements are used in view of their high accuracy. In the general case that independent (non-hardware or time integrated *a priori*) receivers are used and each one has a separate oscillator, double differencing observables are formed so that most error sources, namely satellite and receiver clock errors, atmospheric errors, satellite orbit errors as well as line biases caused by different cable lengths, cancel out. The remaining error sources remaining consist of multipath, antenna phase centre offsets and noise, provided that the double difference integer carrier ambiguities are correctly solved.

3. HEADRT+™ ALGORITHM. Attitude estimation in HEADRT+™ is carried out in two phases. The first phase determines the correct double difference carrier phase ambiguities for the antenna vector(s). Then after coordinate transformation from WGS-84 to the local level frame, the attitude parameters are estimated from the quasi-observable vector components. The ambiguity resolution used in HEADRT+™ is based on the Least Squares Ambiguity Search Technique (Hatch 1991). The location of the master antenna is determined using a standard single point position solution approach. Since no attitude information is known *a priori*, the ambiguity search region is defined as a sphere with the origin at the primary antenna location and the radius as the inter-antenna distance. Therefore, the potential position of the secondary antenna should fall on the shell of this sphere. After forming all the double difference ambiguity combinations that fall within the sphere, statistical tests based on double difference residuals and the inter-antenna length check are used to identify the correct ambiguity set (Hoyle et al 2002). Once the inter-antenna vector ambiguities are fixed, the vector components are transformed from WGS-84 into the local level frame. The three Euler attitude parameters are calculated using an implicit least squares estimation to allow for the epoch-by-epoch assessment of the attitude estimates under either static or dynamic mode (Lu 1994). The Kalman filter estimation has also been implemented in the software. The filter is especially effective when the platform dynamics is predictable relative to the carrier phase measurement rate.

4. GPS HARDWARE. The low-cost GPS sensor type selected for this investigation is the CMC Allstar unit, a GPS OEM receiver card manufactured by the Canadian Marconi Company. It is a 12-channel L1 unit that offers competitive performance at a reasonable price (less than $1000 for the raw carrier phase option). The compact size and small power consumption of the receiver make it appropriate for kinematic applications. The receiver can output raw measurements up to 10 Hz through a RS232 port at a baud rate of 38400. The raw binary carrier phase measurement consists of the PRN number, C/A code range, carrier phase, C/N_o and cycle slip counter. The code and carrier phase noise level is of the order of 0·5 m and 1 mm, respectively (Dumaine 1996). The standard low cost antenna used with the Allstar receiver is the AT575-70 antenna, which is an active antenna with a diameter of 5 cm. As discussed by Wang & Lachapelle (2002), the performance of attitude estimation using these low-cost GPS units depends on the platform dynamics and the antenna type used. Recent research (Wang 2003) shows that low-cost antennas that are heavily plagued by phase centre variations and multipath

https://doi.org/10.1017/S0373463303002583 Published online by Cambridge University Press

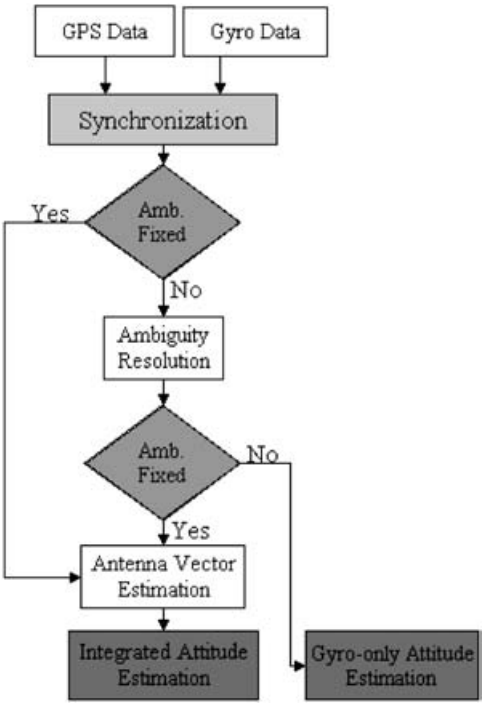

Figure 1. GPS-Rate gyro integration methodology.

that may lead to double differenced carrier phase measurement errors of up to several cm.

5. INTEGRATION METHODOLOGY.

5.1. *General.* Three orthogonally-mounted rate gyroscopes are integrated with the GPS-based system to continuously measure the angular rates of the platform. There are advantages in introducing rate gyros. From an accuracy aspect, as the rate gyros have fairly stable performance over short intervals, their angular rate measurements can effectively reduce GPS-induced high frequency noise in the attitude estimates. During GPS outages and the integer ambiguity resolution process, the attitude variations can be directly estimated from the rate gyro measurements alone, which improves system availability. Once the correct attitude estimates are continuously available using the integrated system, the ambiguity search region can be defined as a small cube based on the known orientation of the antenna array, which accelerates the ambiguity resolution process and increases robustness when outages occur and new satellites come in. The robust estimation of attitude rates in the integrated system also significantly enhances the quality control system in the Kalman filter. As the rate gyro can only provide rate measurements, the initial absolute orientation of the platform has to be derived from carrier phase measurements. Initialization thus requires full GPS availability.

Figure 1 depicts the integration scheme of the integrated system. After data synchronization, the antenna vector components are estimated in the local level

https://doi.org/10.1017/S0373463303002583 Published online by Cambridge University Press

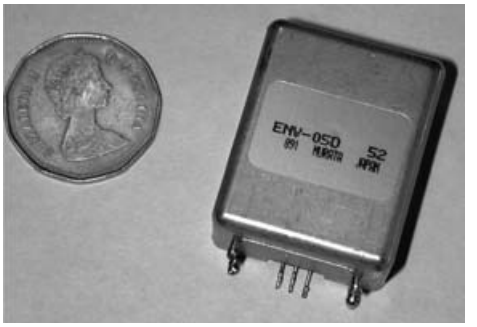

Figure 2. Murata ENV-05D-52 rate gyroscope.

frame once the double differenced ambiguities are correctly determined. Then the antenna vector solutions are fused with rate gyro measurements in a Kalman filter to estimate the attitude parameters. If GPS outages occur after system initialization, the rate gyros provide availability and continuity with a somewhat predictable accuracy degradation.

5.2. *Gyroscope*. The Murata ENV-05D-52 piezoelectric vibrating gyroscope, which is shown in Figure 2, was designed for coarse direction detection in vehicular navigation. Its output is an analogue voltage proportional to the sensed angular rate at a frequency of 2 kHz. The voltage output at zero rate is unit-dependent and ranges from 2·2 to 2·8 V with a mean of 2·5 V. The maximum angular velocity that can be sensed is 80 deg/s. With an increase in angular velocity, the voltage variation can extend 1·5 V in each direction. The temperature drift of this gyro type can reach up to 9 deg/s (Murata 2000). Performance is limited by gyro bias and scale factor drift as well as high frequency noise. Previous research (Hayward et al. 1997, Stephen 2000) has shown that the magnitude of the first two error sources is related to the external temperature, and that simultaneous calibration is very difficult. Biases also drift over time due to hardware self-heating. In this work, the biases are estimated and updated online in the filter when GPS measurements are available. During GPS outages, the bias estimates remain fixed and are used to correct measured angular rates. Compared with the gyro bias, the scale factors are not as sensitive to temperature and their values are closed to 22 mV/°/s within a range of 30°. For this reason, they can be determined *a priori*, provided the temperature does not change greatly during the mission. The high frequency noise in the angular velocity data can be suppressed when averaging the high frequency gyro measurements to 10 Hz for synchronization with the GPS measurements. The rate gyros have also shown limited endurance to shock and vibration. In vehicular attitude determination mode, platform vibration varies significantly depending on the engine, temperature and other factors (e.g. Stephen 2000) and it is next to impossible to develop a valid model to compensate for errors caused by such vibrations.

5.3. *Integration algorithm*. Fusion of the GPS and gyro measurements is achieved with an extended centralized Kalman filter which allows for tight data integration and better error detection. After determining the double difference ambiguities and inter-antenna vectors, the GPS observables in the Kalman filter consist

https://doi.org/10.1017/S0373463303002583 Published online by Cambridge University Press

of inter-antenna vector components in the local level frame. The rate gyro measurements are the angular rates around the three axes in the body frame (ω_x, ω_y, ω_z). The filter 9-state vector X consists of three gyro biases, three Euler attitude parameters and their angular rates:

$$X=(\psi \quad \theta \quad \varphi \quad \dot{\psi} \quad \dot{\theta} \quad \dot{\varphi} \quad \delta\omega_z \quad \delta\omega_x \quad \delta\omega_y)^T. \tag{2}$$

The design matrix **H** for the GPS vector components is the partial derivative of the rotation matrix with respect to the state vector:

$$\underset{3n\times 9_{gps}}{\mathbf{H}} = \frac{\partial \mathbf{R}}{\partial \mathbf{X}}. \tag{3}$$

n is the number of antenna vectors that have been estimated from the GPS measurements.

The relationship between angular rates, attitude angles and gyro biases is given by the following equation, where $s(\ )$ and $c(\ )$ denote the sine and cosine functions:

$$\begin{pmatrix} \omega_z \\ \omega_x \\ \omega_y \end{pmatrix} = \begin{pmatrix} c(\varphi)c(\theta) & -s(\theta) & 0 \\ s(\varphi)c(\theta) & c(\varphi) & 0 \\ -s(\theta) & 0 & 1 \end{pmatrix} \cdot \begin{pmatrix} \dot{\psi} \\ \dot{\theta} \\ \dot{\varphi} \end{pmatrix} + \begin{pmatrix} \delta\omega_z \\ \delta\omega_x \\ \delta\omega_y \end{pmatrix} \tag{4}$$

The design matrix for the angular rate measurements can be formed as:

$$H_{gyro} = \begin{pmatrix} 0 & 0 & 0 & c(\varphi)c(\theta) & -s(\theta) & 0 & 1 & 0 & 0 \\ 0 & 0 & 0 & s(\varphi)c(\theta) & c(\varphi) & 0 & 0 & 1 & 0 \\ 0 & 0 & 0 & -s(\theta) & 0 & 1 & 0 & 0 & 1 \end{pmatrix} \tag{5}$$

A random walk model is used to predict the angular rates and gyro biases in the Kalman filter. Therefore, the transition matrix Φ can be derived from the dynamics model as:

$$\phi = \begin{pmatrix} 1 & 0 & 0 & dt & 0 & 0 & 0 & 0 & 0 \\ 0 & 1 & 0 & 0 & dt & 0 & 0 & 0 & 0 \\ 0 & 0 & 1 & 0 & 0 & dt & 0 & 0 & 0 \\ 0 & 0 & 0 & 1 & 0 & 0 & 0 & 0 & 0 \\ 0 & 0 & 0 & 0 & 1 & 0 & 0 & 0 & 0 \\ 0 & 0 & 0 & 0 & 0 & 1 & 0 & 0 & 0 \\ 0 & 0 & 0 & 0 & 0 & 0 & 1 & 0 & 0 \\ 0 & 0 & 0 & 0 & 0 & 0 & 0 & 1 & 0 \\ 0 & 0 & 0 & 0 & 0 & 0 & 0 & 0 & 1 \end{pmatrix}. \tag{6}$$

The process noise of the dynamic model, which is represented by the **Q** matrix in the Kalman filter, has to be appropriately modelled in order to achieve a high accuracy for the attitude parameter estimation. The mathematical expression for the process

https://doi.org/10.1017/S0373463303002583 Published online by Cambridge University Press

noise is:

$$\mathbf{Q}=\begin{pmatrix} \frac{\sigma_{\dot\psi}^2}{3}dt^3 & 0 & 0 & \frac{\sigma_{\dot\psi}^2}{2}dt^2 & 0 & 0 & 0 & 0 & 0 \\ 0 & \frac{\sigma_{\dot\theta}^2}{3}dt^3 & 0 & 0 & \frac{\sigma_{\dot\theta}^2}{2}dt^2 & 0 & 0 & 0 & 0 \\ 0 & 0 & \frac{\sigma_{\dot\varphi}^2}{3}dt^3 & 0 & 0 & \frac{\sigma_{\dot\varphi}^2}{2}dt^2 & 0 & 0 & 0 \\ \frac{\sigma_{\dot\psi}^2}{2}dt^2 & 0 & 0 & \sigma_{\dot\psi}^2 & 0 & 0 & 0 & 0 & 0 \\ 0 & \frac{\sigma_{\dot\theta}^2}{2}dt^2 & 0 & 0 & \sigma_{\dot\theta}^2 & 0 & 0 & 0 & 0 \\ 0 & 0 & \frac{\sigma_{\dot\varphi}^2}{2}dt^2 & 0 & 0 & \sigma_{\dot\varphi}^2 & 0 & 0 & 0 \\ 0 & 0 & 0 & 0 & 0 & 0 & \sigma_{w_x}^2 & 0 & 0 \\ 0 & 0 & 0 & 0 & 0 & 0 & 0 & \sigma_{w_y}^2 & 0 \\ 0 & 0 & 0 & 0 & 0 & 0 & 0 & 0 & \sigma_{w_z}^2 \end{pmatrix} \tag{7}$$

The variance of the attitude rates in the above equation depends largely on the dynamic constraint in the Kalman filter. The numerical value of the variance of the gyro bias represents the stability of the gyro bias drift. In vehicular attitude determination, the sigma of the angular rate and gyro bias in the **Q** matrix is empirically selected as 20 °/s and 6 °/s, respectively.

During GPS outages, no antenna vector solutions are available and the attitude parameters are estimated solely from the rate gyro data by which the platform rotation can be determined by integrating the estimated attitude rates. With the knowledge of the initial platform orientation since the last GPS outage, the three Euler angles are calculated as:

$$\begin{pmatrix}\psi\\ \theta\\ \varphi\end{pmatrix}_{K+1}=\begin{pmatrix}\psi\\ \theta\\ \varphi\end{pmatrix}_{K}+dt\,.\begin{pmatrix}\dot\psi\\ \dot\theta\\ \dot\varphi\end{pmatrix}. \tag{8}$$

The attitude rates are computed directly from the gyro measurements after compensating for gyro biases as:

$$\begin{pmatrix}\dot\psi\\ \dot\theta\\ \dot\varphi\end{pmatrix}=\begin{pmatrix}0 & \frac{s(\varphi)}{c(\theta)} & \frac{c(\varphi)}{c(\theta)}\\ 0 & c(\varphi) & -s(\varphi)\\ 1 & s(\varphi)t(\theta) & c(\varphi)t(\theta)\end{pmatrix}\begin{pmatrix}\omega_y-\delta\omega_y\\ \omega_x-\delta\omega_x\\ \omega_z-\delta\omega_z\end{pmatrix}. \tag{9}$$

From this equation, one can see that the attitude rate estimation is related not only to the rate gyro measurements, but to the gyro bias and attitude parameter estimation as well. The attitude estimate performance during GPS outages also rests on the length of the outages. Since there is no GPS data to update the gyro bias online during the outage intervals, the gyro bias estimates are kept fixed and degrade due to bias drift over time. Compensation for gyro biases is less effective as GPS outage intervals increase, which leads to a drift in the attitude parameters as well.

5.4. *Quality control.* As discussed in the previous section, the GPS input in the Kalman filter are the inter-antenna vector solutions after ambiguity resolution. It is possible to use a quality control system based on innovation sequences to check the validity of the vector solutions before attitude estimation. The innovation sequences v_k^- are the differences between the actual observations Z_k and the predicted

https://doi.org/10.1017/S0373463303002583 Published online by Cambridge University Press

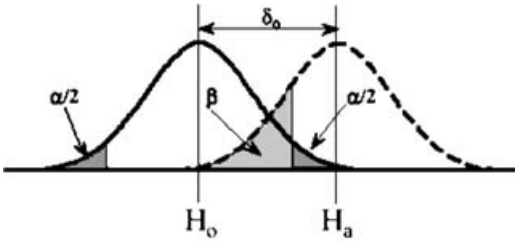

Figure 3. Type I/II errors.

observations based on the predicted state $\hat{x}_k^-$ in the filter (Teunissen and Salzman 1988).

$$v_k^- = z_k - f(\hat{x}_k^-). \tag{10}$$

where $f(\ )$ is the function model, which is the rotation matrix multiplied by antenna vectors in the body frame. Under normal conditions, the innovation sequences have a zero-mean Gaussian white noise sequence with known variance. In the presence of erroneous measurements, such assumptions are no longer valid, and the innovation sequences deviate from the zero mean and white noise properties. Thus some statistical tests can be conducted to detect and identify outliers or faults in the measurements.

Firstly, an overall model test is conducted to detect the errors in the measurement vector. The test statistics in this global test are given as:

$$T_k = v_k^{-T} C_{x_{v_k}^-}^{-1} v_k^- \sim \chi_a^2(m, 0) \tag{11}$$

where m is the number of observations taken at time k, $C_{x_k^-}$ is the covariance matrix of the innovation and χ_α^2 is the Chi-square probability with a significance level of α. If the global test is rejected, the system error can be identified with the one-dimensional local slippage test:

$$w_{ik} = \frac{l_i^T C_{v_k^-}^{-1} v_k^-}{\sqrt{l_i^T C_{v_k^-}^{-1} l_i}} \sim \mathrm{N}(0, 1) \tag{12}$$

where $l_i = (0, \ldots 0_{i-1},\ 1_i,\ 0_{i+1}, \ldots, 0)^T$ for $i = 1, \ldots, m$ and N(0, 1) is the normal distribution. When implementing statistical testing to identify outliers in the measurements, two types of errors may be made. The first type (Type I) is rejecting a good measurement. The probability associated with this type of error is denoted by α. If a bad measurement is accepted by the test, a Type II error occurs. The probability of a Type II error is expressed as β. Given the probability values of Type I and Type II errors, the Minimum Detectable Blunder (MDB) or protection level can be calculated as the ability to detect errors in the system as

$$|\nabla z_i| = \frac{\delta_0}{\sqrt{l_i^T C_{v_k^-}^{-1} l_i}} \tag{13}$$

where δ_0 is a function of α and β, as shown in Figure 3. In the presence of strong multipath, the identification test may be too sensitive and will sometimes lead to a

https://doi.org/10.1017/S0373463303002583 Published online by Cambridge University Press

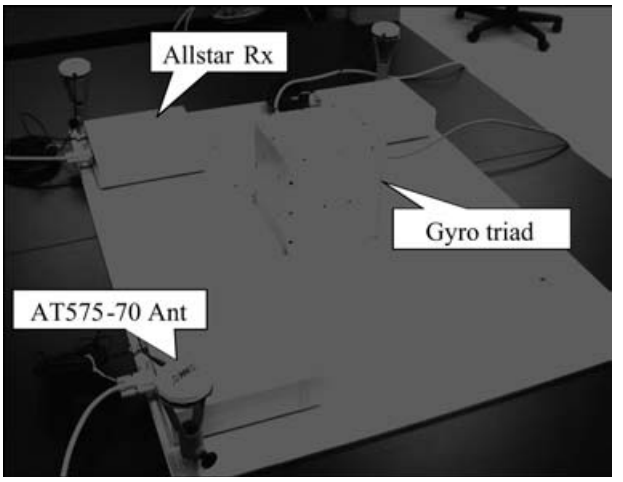

Figure 4. GPS/Rate gyro integrated system for static test.

false alarm (Lu 1991). In order to alleviate this problem, a further step was introduced by comparing the innovations with the MDB. If the innovation is larger than the MDB, the measurement is considered in error, otherwise it is considered a false alarm.

5.5. *Gyro aiding ambiguity resolution*. Once the double difference ambiguities for inter-antenna vectors are fixed, the attitude parameters can be obtained from the integrated Kalman filter solution or the gyro-only solution at each epoch. With the knowledge of the antenna array configuration, the 3D inter-antenna vector components in the local level frame can be calculated based on the approximate attitude information as:

$$\begin{pmatrix} x_{ll} \\ y_{ll} \\ z_{ll} \end{pmatrix} = \mathbf{R}_b^{ll} \begin{pmatrix} x_b \\ y_b \\ z_b \end{pmatrix} \tag{14}$$

where $\mathbf{R}_b^{ll}$ is the rotation matrix from the body frame to the local level and is the transpose of $\mathbf{R}_{ll}^b$ in Equation 1.

After transforming the antenna vector from the local level into earth-fixed frame, the coordinates of the secondary antenna in WGS-84 with respect to the primary antenna can be easily estimated. The search space for the secondary antenna can be defined as a cube with the origin at the estimated primary antenna location and the side of the estimation uncertainty. Then all the candidate double difference ambiguity combinations that fall into the cubic search volume can be formed. During the ambiguity identification process, the known location of the secondary antenna can also be used as an extra constraint to select the true ambiguity set. The gyro-aided ambiguity resolution scheme is very powerful as it can dramatically reduce the candidate ambiguity sets compared to the sphere region that has to be used for the GPS-only case. For an inter-antenna distance of 1 m, the number of ambiguity combinations that fall in the sphere is about 1400. The number decreases to 12-20 using the

https://doi.org/10.1017/S0373463303002583 Published online by Cambridge University Press

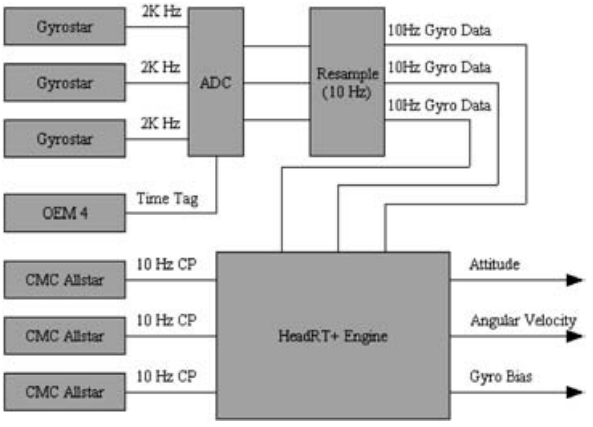

Figure 5. Integrated system setup.

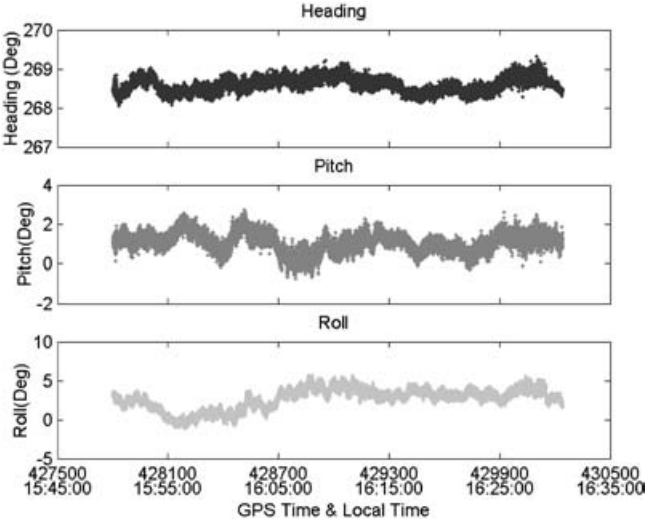

Figure 6. GPS-only attitude estimates – Static test.

cube definition with a side of 20 cm. With such a small number of candidate combinations, the integer ambiguities can always be successfully determined within a few epochs in the preliminary static test.

6. STATIC TESTING. A 45-minute static test was carried out to investigate the performance of the proposed system. As shown in Figures 4 and 5 the system was set up using three GPS units and three rate gyros. The distances between the three AT575-70 GPS antennas deployed were 0·8 and 0·6 m, respectively. The rate gyro voltage pulse outputs were digitized in an A/D converter and synchronized with GPS time, temporarily provided by a separate dedicated GPS unit. The 2 kHz digital rate gyro angular rates were averaged to 10 Hz for data synchronization and noise suppression. The attitude results using the GPS data only are shown in Figure 6. The heading, pitch and roll RMS values with respect to the estimated

https://doi.org/10.1017/S0373463303002583 Published online by Cambridge University Press

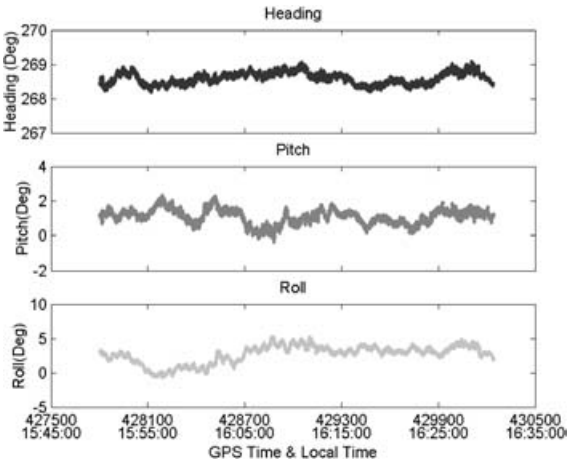

Figure 7. GPS/Rate gyro attitude estimates – Static test.

means are 0·19°, 0·53° and 1·37°, respectively. The attitude parameter estimates show low frequency fluctuations, which are due to multipath and antenna phase centre variations. The filter process cannot entirely remove the high noise, partly as a result of the short inter-antenna distances. Then the rate gyro measurements were integrated with the GPS data. During the process, it was found that even after gyro data down-sampling to 10 Hz, the gyro bias estimates were not stable due to high noise level in the angular rate measurement. A smoothing process with a window length of 20 seconds was introduced to suppress the noise effect on these estimates since the gyro bias drifts smoothly over time. The resulting estimated attitude parameters are shown in Figure 7. The heading, pitch and roll RMS values with respected to the estimated means are 0·17°, 0·43° and 1·32°, respectively. These values are slightly smaller than the corresponding GPS-only values because the rate gyro measurements contribute to smoothing the high frequency GPS-only noise over very short intervals, as can also be seen by comparing Figure 7 and 6. The attitude rate estimates from the GPS-only and integrated systems are listed in Table 1. The estimates have zero means since the system is not moving. However, with the aid of rate gyro measurements, the RMS values improve by more than 50%. This enhancement contributes to improving the quality control system based on innovation sequences, as shall be seen later.

In this low-cost integration scheme, the precise estimation of gyro biases is imperative as the performance of gyro coasting during GPS outages relies highly on their estimates. As the platform is kept stationary during this static test, the voltage output variations were solely due to the gyro bias drifts and the measurement noise. In Figure 8, the bold lines represent the variation patterns of the actual gyro biases contaminated by noise and the grey lines represent the corresponding estimates from the Kalman filter. The three estimated gyro biases tightly coincide with the true values. With the aid of rate gyros, the reliability of the attitude rate estimates is dramatically improved. The enhancement of attitude rate estimation increases the accuracy of innovation sequence testing and therefore leads to smaller Minimum Detectable Blunders (MDBs). The statistical external reliability, which represents the effect of MDBs on the estimated parameters, is thus enhanced as can be seen in

https://doi.org/10.1017/S0373463303002583 Published online by Cambridge University Press

Table 1. Attitude rate estimation from different systems (Unit: deg/sec).

System	Mean/RMS		
	Heading rate	Pitch rate	Roll rate
GPS	0·00/0·06	0·00/0·09	0·00/0·09
GPS/gyro	0·00/0·03	−0·01/0·04	0·00/0·04

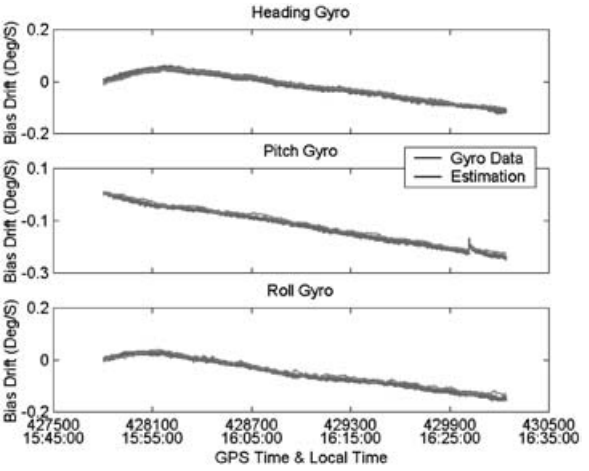

Figure 8. Gyro bias estimation.

Figure 9. The grey and bold lines show the external reliability or protection level for the GPS-only and GPS/rate gyro integrated system. These values are the errors that could occur and go undetected, should actual measurement errors reach values close to the MBDs. By introducing the rate gyro measurements, the external reliability of attitude parameters improves dramatically. The variation in external reliability values over time is caused by changes in the number and geometry of the satellites. In order to examine the coasting capability of the rate gyros when no GPS solutions are available, five GPS outages with lengths ranging from 20 to 60 seconds were simulated in this data set. During these outages, the attitude parameters were estimated using solely the angular rate measurements from the rate gyros. Compared with the attitude results from the integrated system, the differences shown in Figure 10 are indicative of the estimated errors due to the free run of the rate gyros. For the heading and pitch components, the errors are always within 1° even over 60 seconds outages. The roll errors are slightly larger and grow to more than 2° in one 60-second outage. The accuracy of the gyro bias estimates, as well as the length of the outages affects the coasting performance of the rate gyros. The roll errors during the first 60-second outage (2nd gap) is larger than the corresponding errors in the second 60-second outage (5th gap), which indicates that the gyro bias estimate in the second case is somewhat better than that during the second gap. This performance level is the best that can be achieved for this particular triad of rate gyros since the system is in static mode and free from vibrations and other dynamic effects. Performance differences between different sets of rate gyros can also be significant as many gyros perform better than minimum specifications.

https://doi.org/10.1017/S0373463303002583 Published online by Cambridge University Press

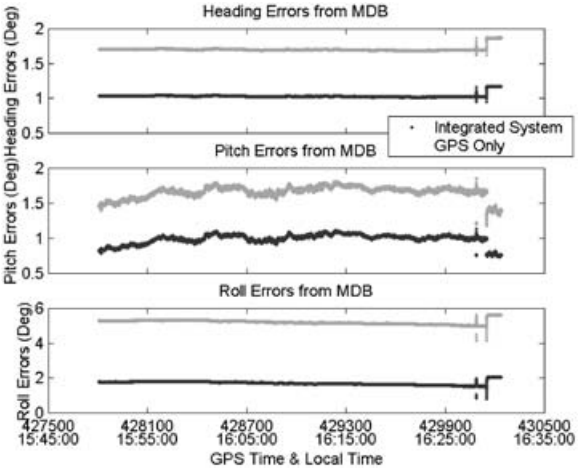

Figure 9. External reliability/Protection level.

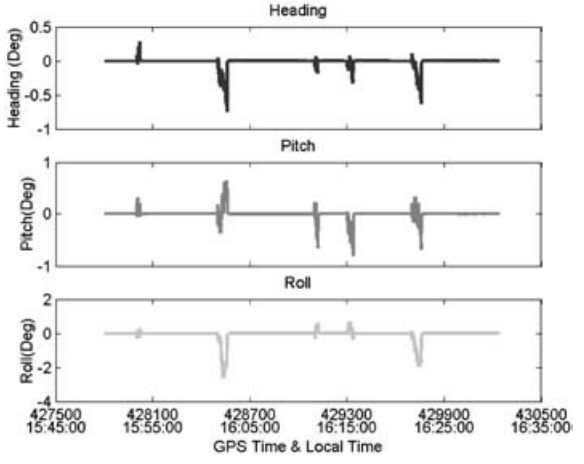

Figure 10. Effect of GPS outages on GPS/Rate gyro system – Static test.

7. KINEMATIC TESTING. In this vehicular test, the GPS component of the system consisted of four Allstar units. The inter-antenna vectors of the co-planar antenna system, shown in Figure 11, were 0·6, 0·8 and 1·0 m, respectively. A NovAtel BlackDiamond™ GPS/INS system was used to independently obtain reference attitude values. The SAINT™ (Satellite and Inertial Navigation Technique) software was used to process the GPS/INS data (Petovello 2003). The standard deviations of the GPS/INS derived attitude components were always within three arcmins. In addition, a high-performance/high cost GPS multi-antenna attitude system consisting of NovAtel Beeline™ receivers and four NovAtel 501 antennas was used to allow further comparisons between different GPS receiver grades. The antennas and rate gyros were installed on the roof of a 2001 Dodge Grand Caravan test vehicle, as shown in Figure 11. During the 16-minute test run, the average velocity of the vehicle was about 70–90 km/hr, which introduced some vibration and jerk on the system. The roll and pitch were consistently below 8°. The various

https://doi.org/10.1017/S0373463303002583 Published online by Cambridge University Press

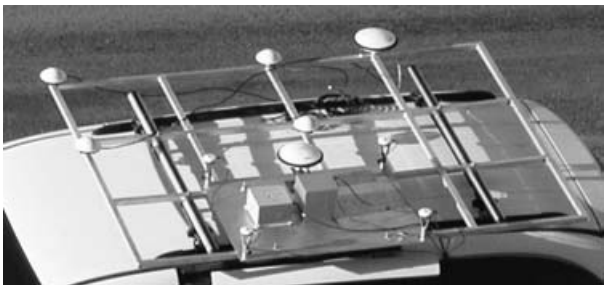

Figure 11. Antenna setup – Kinematic test.

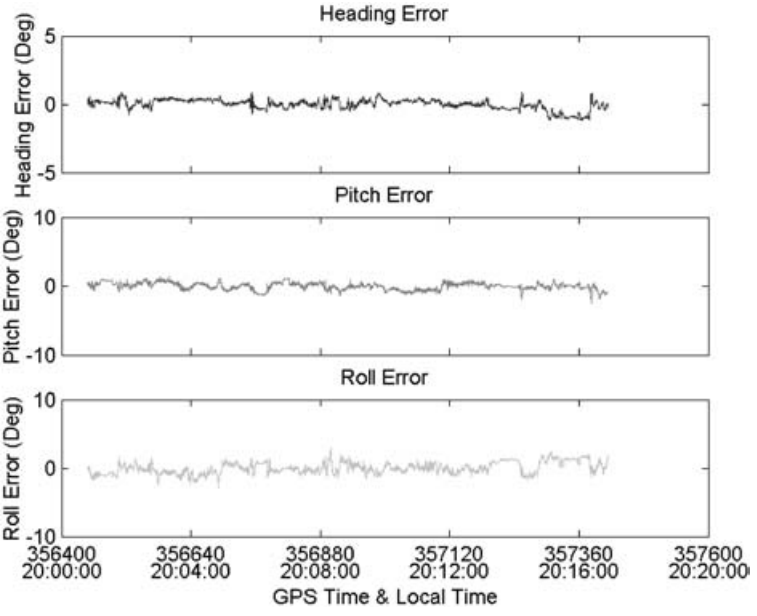

Figure 12. Beeline™/Rate gyro attitude estimation errors – Kinematic test.

attitude platforms were not perfectly aligned with respect to each other, their misalignments being of the order of 1° to 2°. The misalignments were estimated in static mode using standard techniques (e.g., Lu 1994).

The carrier phase measurements of the Beeline™ system were found to be of a superior quality, and the true double difference ambiguities were solved instantaneously at the start of the test. No cycle slips occurred or were detected and the integer ambiguities for the three inter-antenna vectors were correctly fixed during the entire test run. After misalignment angles compensation, the estimated attitude parameters were compared with the reference GPS/INS values and the results are shown in Figure 12. The heading, pitch and roll RMS differences are 0·37°, 0·52° and 0·85°, respectively, while the corresponding mean differences are −0·01, 0·01 and 0·00, respectively. The latter values are an indication of the high quality of the Beeline™ units and 501 antennas. Given the short inter-antenna distances, the RMS agreement is fully satisfactory. Since accurate attitude estimates are available continuously during the test, the rate gyro biases can be precisely estimated using the Beeline™

https://doi.org/10.1017/S0373463303002583 Published online by Cambridge University Press

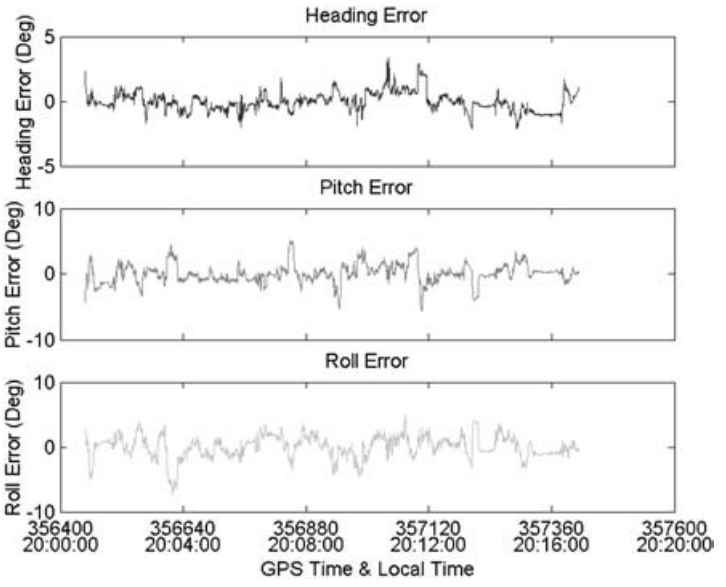

Figure 13. Allstar/Rate gyro attitude estimation errors – Kinematic.

units. These estimates will be used as the reference values when examining the gyro bias estimation results of the low-cost integrated system.

As expected, the carrier phase measurements using the low-cost receivers and AT575-70 antennas are severely affected by multipath and antenna phase centre variations as well as cycle slip occurrences. Double difference residuals reached 7–8 cm even though the integer ambiguities were correctly determined. This kind of noisy carrier phase measurements not only results in a poor attitude component estimation accuracy, but also leads to integer ambiguity resolution and cycle slip detection difficulties. A residual check is used in HEADRT+™ to distinguish the correct ambiguity set as well as to detect small cycle slips (0·5 or 1 cycle). The large carrier phase measurement errors due to antenna effects under kinematic conditions makes this check too sensitive if the tolerance selected is as small as that used for the Beeline™ units. However, choosing a higher threshold for the residual check is risky as it may lead to wrong ambiguity sets passing through the ambiguity distinguishing process. In this test, the above criterion was optimistic in order to reject any incorrect ambiguity set since the rate gyros can ensure availability in the case of no GPS solutions. As a result of choosing a small tolerance, the fixed double difference ambiguities were frequently identified as erroneous and the ambiguity resolution restarted often due to the large double difference phase residuals. Even though false detections occur, they do not affect the attitude estimation performance provided the correct double difference ambiguities can be resolved again instantaneously. When the sphere search volume is used for the ambiguity resolution process, the entire search process takes 10 to 20 seconds and 20% of the sets are identified as erroneous by the quality control system. In comparison to the sphere volume method, the cube search region definition significantly reduces the search volume and the number of candidate ambiguities, resulting in a fast and reliable ambiguity resolution. In this case, the integer ambiguities could be correctly selected in less than 1 s 91% of the time. 88·4% of the

https://doi.org/10.1017/S0373463303002583 Published online by Cambridge University Press

attitude solutions are estimated from GPS/rate gyro measurements and the remaining 11·6% from rate gyro measurements only. The lower availability of integrated solutions is caused mostly by multipath and antenna phase centre variations, in addition to the tight threshold used for residual testing.

The Allstar/rate gyro estimated attitude components are compared to the GPS/INS reference values in Figure 13. The mean differences are $-0{\cdot}04^\circ$, $0{\cdot}03^\circ$ and $-0{\cdot}01^\circ$ in heading, pitch and roll, respectively. The corresponding RMS differences are $0{\cdot}73^\circ$, $1{\cdot}46^\circ$ and $1{\cdot}74^\circ$, respectively. Even through most of the attitude errors are within a two-sigma limit, the maximum heading, pitch and roll differences reach $3{\cdot}38^\circ$, $5{\cdot}50^\circ$ and $7{\cdot}26^\circ$, respectively. The longest coasting period using rate gyro data only is 12·9 s, which leads to a 2-degree error in each attitude component. Many of the large estimation errors are due to multipath and antenna phase variations. Most if not all cycle slip occurrences can be identified using a combination of the phase prediction method, residual checking and the innovation sequences, since the dramatic change in residuals or vector solutions due to cycle slips is easy to detect by these methods. However, the quality control system based on innovation sequences is insensitive to low frequency antenna phase centre variations and multipath. Using a smaller tolerance in the residual check may have an impact on rejecting GPS antenna vector solutions that are contaminated by strong multipath and large antenna phase centre offsets in attitude, but the lower availability of GPS solutions would in this case leads to larger errors since the rate gyro errors grow quickly in coasting mode.

8. CONCLUSIONS.

The use of low-cost piezoelectric vibrating rate gyros significantly enhances the availability and reliability performance of low-cost GPS-based attitude determination systems. With the aid of continuous angular rate measurements, the high frequency noise in attitude estimates can also be slightly reduced, thereby improving short term accuracy. Platform attitude estimates can be determined by integrating the gyro angular rate measurements over time during GPS outages. The Kalman filter prediction process is enhanced compared with a GPS-only system, which improves error detection capability and increases error protection level. The test results show that low cost antenna phase centre variations and multipath have a severe impact on carrier phase measurements and restrict the performance of the system. Calibration of antenna phase centre variations or the use of higher grade antennas to mitigate the above two errors would significantly improve performance. Higher performance rate gyros for the GPS/gyro integration would also improve coasting capability during extended GPS outages, but with increased cost.

REFERENCES

Cohen, C.E. (1992) *Attitude Determination Using GPS*, Ph.D. thesis, Stanford University.

Dumaine, M. (1996) *High Precision Attitude Using Low-cost GPS Receivers*, Proceedings of ION GPS 1996, Kansas City, September 17–20, Institute of Navigation, pp. 1029–1035.

Gebre-Egziabher, D., Hayward, C. and Powell, D. (1998) A Low-Cost GPS/Inertial Attitude Heading Reference System (AHRS) for General Aviation Applications, Proc. of 1998 IEEE Position, Location and Navigation Symposium, Palm Springs, CA, http://einstein.stanford.edu/gps/PDF/cheap_ahrs_4_ga_dge98.pdf

Hatch, R. (1991) Instantaneous Ambiguity Resolution, *Proceedings of the IAG International Symposium 107 on Kinematic Systems in Geodesy*, *Surveying and Remote Sensing*, Banff, Canada, September, 1990, Springer-Verlag, New York, pp. 299–308.

Hayward, R.C., Gebre-Egziabher, D., Schwall, M., Powell, D. and Wilson, J. (1997) Inertially Aided GPS Based Attitude Heading Reference System (AHRS) for General Aviation Aircraft, *Proc. of ION GPS97*, Kansas City, MO, September, 1997, pp. 289–298.

Hoyle, V., Lachapelle, G., Cannon, M.E. and Wang, C. (2002) Low-Cost GPS Receivers and their Feasibility for Attitude Determination, *Proc. of GPS NTM02*, The Institute of Navigation, San Diego, CA, pp. 226–234.

Lu, G. (1991) Quality Control for Differential Kinemaitc GPS Positioning, M.Sc. thesis, Department of Geomatics Engineering Report No. 20042, University of Calgary, http://www.geomatics.ucalgary.ca/links/GradTheses.html

Lu, G. (1994) Development of a GPS Multi-Antenna System for Attitude Determination, Ph.D. thesis, Department of Geomatics Engineering Report No. 20073, University of Calgary, http://www.geomatics.ucalgary.ca/links/GradTheses.html

Murata (2000) Technologies Used for Ceramic Bimorph Gyroscopes, http://www.murata.com/articles/9089.html

Petovello, M. (2003) Real-time Integration of a Tactical-Grade IMU and GPS for High-Accuracy Positioning and Navigation, Ph.D. thesis, UCGE Report No. 20173, Department of Geomatics Engineering, University of Calgary, http://www.geomatics.ucalgary.ca/links/GradTheses.html

Stephen, J. (2000) Development of a Multi-sensor GNSS Based Vehicle Navigation System, M.Sc. thesis, Department of Geomatics Engineering Report No. 20140, University of Calgary, http://www.geomatics.ucalgary.ca/links/GradTheses.html

Teunissen, P.J.G. and Salzman, M.A. (1988) *Performance Analysis of Kalman Filters*, Reports of the Faculty of Geodesy, Delft University of Technology, Delft, The Netherlands.

Wang, C. (2003) Development of a Low-cost GPS-based Attitude Determination System, M.Sc. thesis, Department of Geomatics Engineering Report No. 20175, University of Calgary, http://www.geomatics.ucalgary.ca/links/GradTheses.html

Wang, C. and Lachapelle, G. (2002) GPS Attitude Determination Reliability Performance Improvement Using Low Cost Receivers. *Journal of Global Positioning Systems*, **1**, 2, pp. 85–95.